

MPG: A Multi-ingredient Pizza Image Generator with Conditional StyleGANs

Fangda Han
Rutgers University
Piscataway, NJ, USA
fh199@cs.rutgers.edu

Guoyao Hao
Rutgers University
Piscataway, NJ, USA
gh343@scarletmail.rutgers.edu

Ricardo Guerrero
Samsung AI Center
Cambridge, UK
r.guerrero@samsung.com

Vladimir Pavlovic
Rutgers University
Piscataway, NJ, USA
vladimir@cs.rutgers.edu

Abstract

*Multilabel conditional image generation is a challenging problem in computer vision. In this work we propose **Multi-ingredient Pizza Generator (MPG)**, a conditional Generative Neural Network (GAN) framework for synthesizing multilabel images. We design MPG based on a state-of-the-art GAN structure called StyleGAN2, in which we develop a new conditioning technique by enforcing intermediate feature maps to learn scalewise label information. Because of the complex nature of the multilabel image generation problem, we also regularize synthetic image by predicting the corresponding ingredients. To verify the efficacy of MPG, we test it on **Pizza10**, which is a carefully annotated multi-ingredient pizza image dataset. MPG can successfully generate photo-realist pizza images with desired ingredients. The framework can be easily extend to other multilabel image generation scenarios.*

1. Introduction

Table 1. Glossary of terms.

Term	Description
<i>MPG</i>	Multi-ingredient Pizza Generator
<i>SLE</i>	Scalewise Label Encoder
<i>CR</i>	Classification Regularizer
Pizza10	Proposed multi-ingredient annotated pizza dataset

Generative Adversarial Networks [8] (GAN) are a type of generative models that can create high-fidelity images [18, 17, 2] by alternatively optimizing its two components: generator and discriminator. We exploit the capacity of GAN models for solving the problem of generating food images conditioned on multiple ingredients. Food im-

ages are naturally complex since ingredients usually have different colors and shapes; even the same ingredient can have different colors with varying methods of cooking (e.g. pepperoni will become darker with longer cooking time or higher cooking temperature). Moreover, ingredients in food images are usually mixed together, and therefore, the model has to learn to arrange the ingredients correctly on an image.

Previous works on food image generation either use images as input [15, 29] or generate blurry images [10]. We propose a conditional generative adversarial network called Multi-ingredient Pizza Generator (*MPG*) inspired by [19]. *MPG* first encodes the ingredients into different scale-specific embeddings, injected into the synthesis network together with a “style noise” to create images. These same ingredient embeddings are also injected into the discriminator to guide the discrimination process.

Our main contributions are: (1) We propose a novel multilabel conditional GAN framework that is based on StyleGAN2 [19]. This new framework incorporates a Scalewise Label Encoder (*SLE*) and a Classification Regularizer (*CR*) that guide the generator in the synthesis of the desired ingredients. (2) We create a new dataset **Pizza10** from pizza-GANdata [29], by relabeling using a subset of the ingredient labels. After re-annotation, these labels are able to perform more accurate in the multilabel classification and image retrieval tasks.

The remainder of this manuscript is organized as follows: **Sec. 2** introduces the related works including GAN, conditional GAN, food generation and multilabel image generation. **Sec. 3** presents our conditional StyleGAN framework *MPG* as well as the Scalewise Label Encoder (*SLE*) and Classification Regularizer (*CR*). **Sec. 4** describes our motivation to create **Pizza10** dataset and illustrates the improvement from the dataset reframing process. **Sec. 5** includes experiments that verify the effectiveness of our framework,

an ablation study, and an assessment of generated images. Finally, in [Sec. 6](#) we summarize our conclusions.

2. Related Works

GANs [8] were proposed in 2014 and originally trained as a two-player min-max game to estimate the true data distribution from samples. In the past few years, GANs have evolved rapidly, improving their ability to generate high-fidelity digital images of compact objects and natural scenes [25, 2, 17], as well as human faces [18, 19]. As GAN training involves two neural networks competing with each other, it is well-known to suffer from instability during training, leading to failure to converge or mode collapse [23, 33]. Techniques proposed to solve these problems include mini-batch normalization [33], R1 regularization [6, 31], Wasserstein loss [1, 9], Spectral Normalization [25] adaptive augmentation [17], etc.

Conditional GAN [24] extends GAN by conditioning generation process with auxiliary information to control the appearance of generated images, e.g. controlling handwriting digit in MNIST [24], natural object or scene category in ImageNet dataset [26], or the category of CIFAR10 dataset [17]. The work proposed by [28] is the closest to our proposed framework. There, the authors apply StyleGAN to the logo generation task. Our task differs substantially from this as we seek to condition on more than a single label (e.g. ingredients); thus, the structures and spatial relationships among labels are far more diverse. Another line of research that uses conditional GANs, aims at conditioning directly with an input image, with the goal of changing its attributes [12, 3] or associated styles [14, 41]. However, it is important to note that the task of our proposed work is more complicated, as we only have labels as the conditioning input, lacking the input image as a strong prior. Finally, image GANs can be conditioned directly on natural language textual descriptions [40, 39, 22]. While, in principle, more general, these approaches in practice work well on objects such as birds or flowers that share similar structures within classes, but tend to fail on complex scene generation, like those in COCO Dataset.

Food Image Generation is usually accomplished using a conditional GAN to attain higher fidelity compared with other generative models like VAEs [21] or Flow [20, 4, 5]. [32] concatenates the embedding from a pretrained text encoder with noise to generate text-based food image. [7] also uses the embedding of a pretrained text encoder but applies the more advanced StackGAN2 [40] to generate food image. [10] also applies StackGAN2 but it regularizes the generated image to retrieve the corresponding text. [37] applies ProgressiveGAN [16] to unsupervised food image generation on four different datasets. However, these works typically result in blurry, low-resolution images with miss-

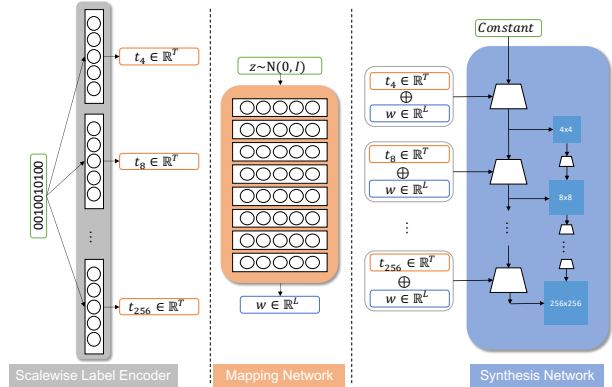


Figure 1. Generator components overview. **Left:** Scalewise Label Encoder (SLE), each scale has its own layers for encoding. **Middle:** Mapping Network. **Right:** Synthesis Network, \oplus means concatenation, notice images at different scales are conditioned with different label embedding

ing details; in contrast, our framework can create images of high fidelity and resolution. [15, 29] apply GANs to transform the food type or add/remove ingredients of a source image. This improves the quality of generated images but requires image-based conditioning; our framework uses labels as input, a significantly weaker form of bias.

Multilabel Image Generation is a special case of text-based image synthesis. [40] uses a stacked multi-scale generator to synthesize images based on text embeddings, [39] extends [40] and synthesize details at different subregions of the image by paying attentions to the relevant words in the natural language description. [30] extends [39] by regularizing the generator and redescribing the corresponding text from the synthetic image. While free text is a potentially stronger signal, it is often corrupted by image-unrelated signals, such as the writing style. On the other hand, while image labels may appear more specific than free-text, the visual diversity of objects described by those labels, such as food ingredients, and the changes in appearance that can arise from interactions of those objects can make the multilabel image generation problem an equal if not greater challenge to that of the caption-to-image task.

3. Methodology

To generate pizza images of high-fidelity, we start from StyleGAN2 [19], one of the state-of-the-art GAN architecture. StyleGAN2 is composed of a generator ([Fig. 1](#)) and a discriminator ([Fig. 2 Left](#)) just like the original GAN, but can generate high-fidelity human faces and objects of up to 1024^2 resolution. There are several techniques involved to improve image quality. (1) The image is generated progressively. Lower-resolution image is generated first and then upsampled and combined with higher-resolution image. (2) There are two sources of noise as the input of the genera-

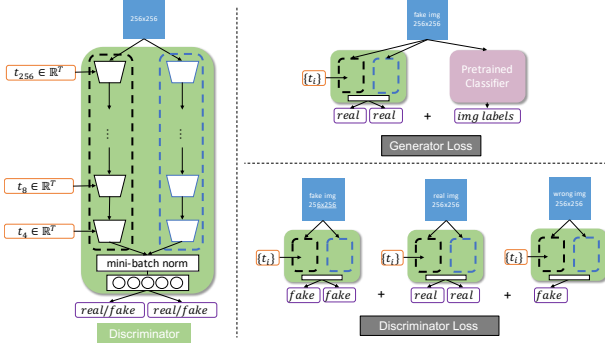


Figure 2. **Left:** Discriminator structure, which contains one branch for conditional output and another branch for unconditional output, notice the label embedding $\{t_i\}$ are reversed to match different scales. **Top right:** Generator Loss, consisting discriminator loss plus Classification Regularizer (CR) loss for fake image. **Bottom right:** Discriminator Loss, consisting three discriminator losses from fake, real and wrong images. Notice the discriminator is trained to distinguish between (txt, real img) and (txt, wrong img)

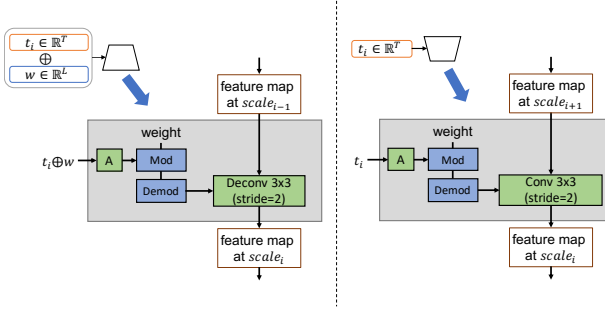


Figure 3. **Left:** Injection block at scale i in the generator (image courtesy [19]). A is a learned affine transformation, ‘weight’ is the learned weight for the deconv layer which is modulated by $t_i \oplus w$ by Mod and $Demod$, refer [19] for more details. **Right:** Injection block at scale i in the discriminator. The same injection idea is applied to the discriminator to inject the label embedding at each scale, here conv layer is used instead of the deconv layer to downsample the feature map

tor, one controls the style and the other controls the detail. The style noise ($z \in \mathcal{N}(0, I)$ in Fig. 1 Middle) and the detail noise (omitted in Fig. 1 because it is irrelevant to our work) are injected into the generator at each scale. The style noise is injected by first passing through a *mapping network* (Fig. 1 Middle) and then transformed to be the weights of the convolutional layers in the generator, therefore achieving a strong control of the image, while the detail noise is injected directly by adding into the output feature map of each convolutional layer as a perturbation. (3) The discriminator is trained with mini-batch normalization [33] to avoid mode collapse of the generator. (4) R1 regularization [31] is applied to improve the robustness of the network.

StyleGAN2 alone has a limited way of controlling the

output image. The authors show that changing the style noise z will result in a shift in human face features (e.g. face outline, skin color, gender etc.). However, given the style noise’s random nature, it is impossible to determine or control specific features in the generated image. In this paper we adjust StyleGAN2 and create Multi-ingredient Pizza Generator (MPG), making it possible to generate pizza images with specific, controllable ingredients and combinations thereof.

Formally, given a binary vector x indicating the ingredient list (Fig. 1 Left), we seek to generate a pizza image y that contains the desired ingredients. We propose to use a model endowed with Scalewise Label Encoder, Classification Regularizer to solve this problem.

3.1. Scalewise Label Encoder

The generator in StyleGAN2 is injected with the style noise z at each scale. Inspired by this, we design *SLE* (Scalewise Label Encoder in Fig. 1 Left) to condition the synthesis network on the binary vector x . *SLE* consists of a sequence of sub-encoders $\{Enc_i(x)\}$ (one for each scale i) and takes x as input to output label embedding $\{t_i\}$ (also one for each scale i). Formally, if the generated image \tilde{y} is of size 256^2 , then we get scalewise label embedding $\{t_i\}$

$$\{t_i\} = SLE(x) = \{Enc_i(x)\}, \quad (1)$$

where $i \in \{4, 8, 16, 32, 64, 128, 256\}$. Enc_i is the encoder at i -th scale. We implement Enc_i by multi-layer perceptron. The mapping network f is kept to provide more diversity to the output image. The label embedding $\{t_i\}$ is then concatenated with the output from the mapping network together as the input of the synthesis network S . We inject $t_i \oplus w$ the same way as in StyleGAN2 (Fig. 3 Left) and generate the output image \tilde{y}

$$w = f(z) \quad (2)$$

$$\tilde{y} = S(\{w, t_i\}). \quad (3)$$

Eq. 1 to Eq. 3 can be further simplified as

$$\tilde{y} = G(x, z), \quad (4)$$

where G is the generator composed of $\{SLE, f, S\}$.

SLE outputs are applied to the discriminator as well, since the discriminator is composed of a sequence of convolutional layers that downsample the input image from high resolution to low resolution, we reverse $\{t_i\}$ and inject each t_i **without** concatenating w at each scale the same way as the generator (Fig. 3 Right). However, during experiments we notice replacing the StyleGAN2 discriminator with the conditional version directly will lead to degeneration in image quality. Inspired by StackGAN2 [40], we extract the convolutional layers in StyleGAN2 discriminator and add it

into the discriminator as the “unconditional branch” (blue dash box in Fig. 2 Left).

Formally, the discriminator D is combined with a conditional branch f_c , an unconditional branch f_{uc} , a mini-batch normalization operation σ and a fully-connected layer F . Given the label embedding $\{\mathbf{t}_i\}$ and input image \mathbf{y} , the outputs can be represented as

$$s_c = D(\{\mathbf{t}_i\}, \mathbf{y}) = F(\sigma(f_c(\{\mathbf{t}_i\}, \mathbf{y}))) \quad (5)$$

$$s_{uc} = D(\mathbf{y}) = F(\sigma(f_{uc}(\mathbf{y}))), \quad (6)$$

where s_c and s_{uc} are conditional output and unconditional output respectively, $i \in \{256, 128, 64, 32, 16, 8, 4\}$. Notice mini-batch normalization is used to correlate samples in a mini-batch in the discriminator to prevent model collapse [33].

Now given a pair of ingredient list and image (\mathbf{x}, \mathbf{y}) , the loss function for the generator can be defined as

$$\max_G = D(\{\mathbf{t}_i\}, G(\mathbf{x}, \mathbf{z})) + \lambda_{uncond} D(G(\mathbf{x}, \mathbf{z})), \quad (7)$$

and the loss for the discriminator is

$$\begin{aligned} \min_D = & D(\{\mathbf{t}_i\}, G(\mathbf{x}, \mathbf{z})) + \lambda_{uncond} D(G(\mathbf{x}, \mathbf{z})) \\ & - D(\{\mathbf{t}_i\}, \mathbf{y}) - \lambda_{uncond} D(\mathbf{y}), \end{aligned} \quad (8)$$

where $\{\mathbf{t}_i\} = SLE(x)$, $\mathbf{z} \in \mathcal{N}(0, I)$, and λ_{uncond} is the weight for unconditional output of the discriminator.

3.2. Classification Regularizer

To help the generator create image with desired ingredients, inspired by [27, 10], we pretrain a multilabel classifier h on pairs of real image and its ingredient list $\{(\mathbf{y}, \mathbf{x})\}$. Then during training the generator, we regularize the generated image $\tilde{\mathbf{y}}$ to predict the correct ingredients \mathbf{x} . The Classification Regularizer (CR) can be formalized as

$$\tilde{\mathbf{x}} = h(\tilde{\mathbf{y}}), \quad (9)$$

this regularizer can be easily combined in the generator loss Eq. 7 as shown in top right of Fig. 2,

$$\begin{aligned} \max_G = & D(\{\mathbf{t}_i\}, G(\mathbf{x}, \mathbf{z})) + \lambda_c D(G(\mathbf{x}, \mathbf{z})) \\ & + \lambda_{clf} BCE(\mathbf{x}, h(\tilde{\mathbf{y}})), \end{aligned} \quad (10)$$

where BCE is binary cross entropy loss and λ_{clf} is the weight for the regularizer.

Except the contents mentioned above, R1 regularization [6] is also kept in the discriminator to penalize the gradient flowed from the image to the output, which has been proved to be helpful in stabilize GAN training process [31]. The final discriminator loss is now

$$\begin{aligned} \min_D = & D(\{\mathbf{t}_i\}, G(\mathbf{x}, \mathbf{z})) + \lambda_{uncond} D(G(\mathbf{x}, \mathbf{z})) \\ & - D(\{\mathbf{t}_i\}, \mathbf{y}) - \lambda_{uncond} D(\mathbf{y}) \\ & + \lambda_{r1} \left(\frac{\partial D(\mathbf{x})}{\partial \mathbf{x}} + \frac{\partial D(\mathbf{x}, \{\mathbf{t}_i\})}{\partial \mathbf{x}} \right). \end{aligned} \quad (11)$$

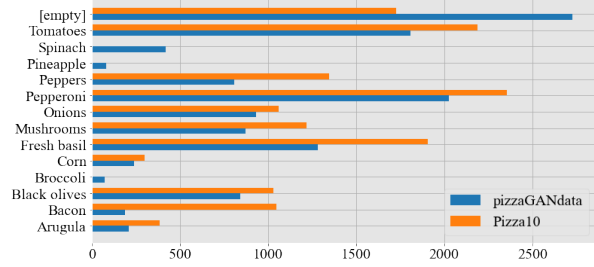


Figure 4. Ingredients distribution comparison between pizzaGANdata and the refined **Pizza10** dataset, ‘[empty]’ represents the number of samples with no ingredients labeled



Figure 5. Illustration of improper labels in pizzaGANdata and the refined labels in **Pizza10** dataset, the difference is highlighted in red (best viewed in color)

Eq. 10 and Eq. 11 summarize all components in the proposed framework MPG . In the following sections, we will use **Pizza10** dataset to verify the efficacy of MPG .

4. Pizza10 Dataset

The performance of neural network models critically depends on the quality of the dataset used to train the models. We begin with the pizzaGANdata [29], which contains 9213 pizza images annotated with 13 ingredients, as shown in Fig. 4. We manually inspected the labeling in this dataset and found a significant portion of it to be mislabeled; we illustrate three instances in Fig. 5. To address this issue, using a custom-created collaborative web platform, we relabeled the dataset and removed three ingredients (*Spinach*, *Pineapple*, *Broccoli*) with fewer number of instances (*Corn* is kept since the distinct color and shape makes it a recognizable ingredient even with fewer samples than *Spinach*). The refined dataset, **Pizza10**, decreases the number of ‘empty samples’ (pizza images with no ingredients labeled) by 40% and increases the number of samples for each ingredient category as shown in Fig. 4. We verify the impact of the curated **Pizza10** on two tasks:

Retrieval. Given an ingredient list as query, we want to retrieve its associated pizza image, we solve this task by following [34]. The ingredient list is treated as a sentence and encoded into a vector of \mathbb{R}^{768} , the text encoder is two-layer-two-head transformer encoder [35] built using HuggingFace[38], and we initialized the embedding from the pre-trained ‘bert-base-uncased’ model on HuggingFace Model Hub. The image is also encoded into a vector of

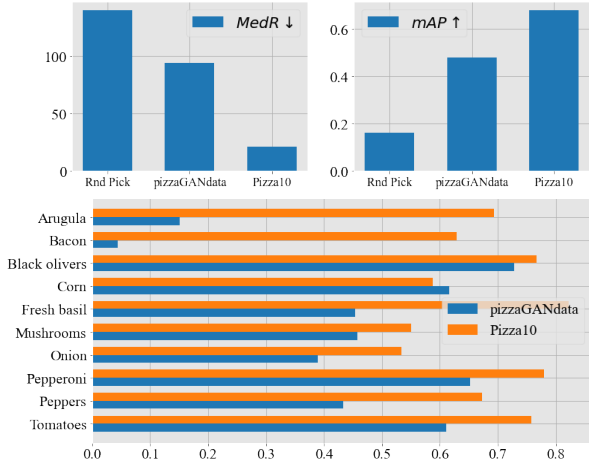


Figure 6. Performance comparison between pizzaGANdata and **Pizza10**. Top left: MedR scores on retrieval task. Top right: mAP scores on multilabel classification task. Bottom: average precision for each ingredient in the classification task. ‘Rnd Pick’ means the scores when we randomly pick answer. ↓ means the lower the better, ↑ means the higher the better

\mathbb{R}^{768} , the image encoder is initialized from ResNet50 [11] with the final fully-connected layer changed to match the output dimension (\mathbb{R}^{768}). The loss is triplet loss with hard-sample mining [36]. We use 60% data for training and leave 40% for testing. After training, we use the median rank (MedR) [34] to measure the performance; the retrieval range is 280, roughly the number of distinct ingredient lists in both datasets. Computed as the median rank of the true positives over all queries, a lower MedR (≥ 1.0) suggests better performance.

Multilabel Classification. Given a pizza image, we seek to predict its ingredients. We initialized the classifier from ResNet50 [11] with the final fully-connected layer changed to match the output dimension (\mathbb{R}^{13} for pizzaGANdata and \mathbb{R}^{10} for **Pizza10**). The loss is a binary cross entropy loss. 80% data are used in training while 20% data are for testing. After training, we use the mean average precision (mAP) as the metric.

The results are shown in Fig. 6. The same model has a big jump in performance on the refined **Pizza10** dataset in both tasks. Upon close inspection, the average precision (AP) for each ingredient increases on most ingredients except *Corn* for the classifier trained on **Pizza10**, therefore demonstrating the importance of careful curating.

5. Experiments

Network Structures. For the generator, *SLE* is composed of a group of sub-encoders, each sub-encoder is a fully-connected layer with ReLU activation. The label embedding dimension $T = 256$, the mapping network is the same as StyleGAN2 except we decrease the style noise dimension

Table 2. Quantitative comparison of performances between baselines and the proposed multi-ingredient Pizza Generator (*MPG*)

Models	Image Size	FID↓	mAP↑
StackGAN2 [40]	256 ²	63.51	0.3219
CookGAN [10]	256 ²	45.64	0.2896
AttnGAN [39]	256 ²	74.47	0.5729
<i>MPG</i>	256 ²	8.43	0.9816

L to 256. The synthesized network is also the same as StyleGAN2 however the input at each scale is now different for matching the scalewise label embedding $\{t_i\}$. For the discriminator, the unconditional branch, mini-batch normalization and fully-connected layer are the same as StyleGAN2, the conditional branch is modified from the injection block of the generator and performs the reversed operation (e.g. injection and downsampling).

Hyper Parameters. For the generator, $\lambda_{uncond} = 1.0$. For the discriminator, $\lambda_{clf} = 1.0$, $\lambda_{r1} = 10$, R1 regularization is performed every 16 mini-batches to balance the training time. The learning rate for both the generator and discriminator is 0.002. The mini-batch size is 24 (need at least 24GB GPU memory).

Configurations. The framework is built using PyTorch 1.7 and trained on four NVIDIA K80 GPUs (each has 12 GB memory), the training takes 6 days to converge for a duration of 2.4M pizza images. Note the number of images needed is much smaller than the StyleGAN model trained on LSUN BEDROOMS, CATS or CARS (see Appendix E in [18]), we believe this is because our dataset is much smaller (e.g. 9213 images in **Pizza10** vs. 3M in LSUN BEDROOMS).

Metrics. We use FID [13] (on 10K images) to assess to the quality of the generated images, a lower FID indicates the generated image distribution is more close to the real image distribution. We use mean average precision [42] (*mAP*) to evaluate the conditioning on the desired ingredients. The multilabel classifier we used is trained on **Pizza10** as shown in Sec. 4 and achieves *mAP* = 0.6804.

5.1. Comparison with Baselines

We compare with three prior works on text-based image generation. **StackGAN2** [40] first extracts text feature from a pretrained retrieval model and then forward through a stacked generator with separate discriminators working at different scales. **CookGAN** [10] uses similar structure as of StackGAN2 and adds a cycle-consistent loss which drives the generated images to retrieve its desired ingredients. **AttnGAN** [39] also shares StackGAN2-like structure, it uses pretrained text encoder to capture the importance of each word and leverages both word-level and sentence-level feature to guide the generation process.

Tab. 2 compares the performance between our model

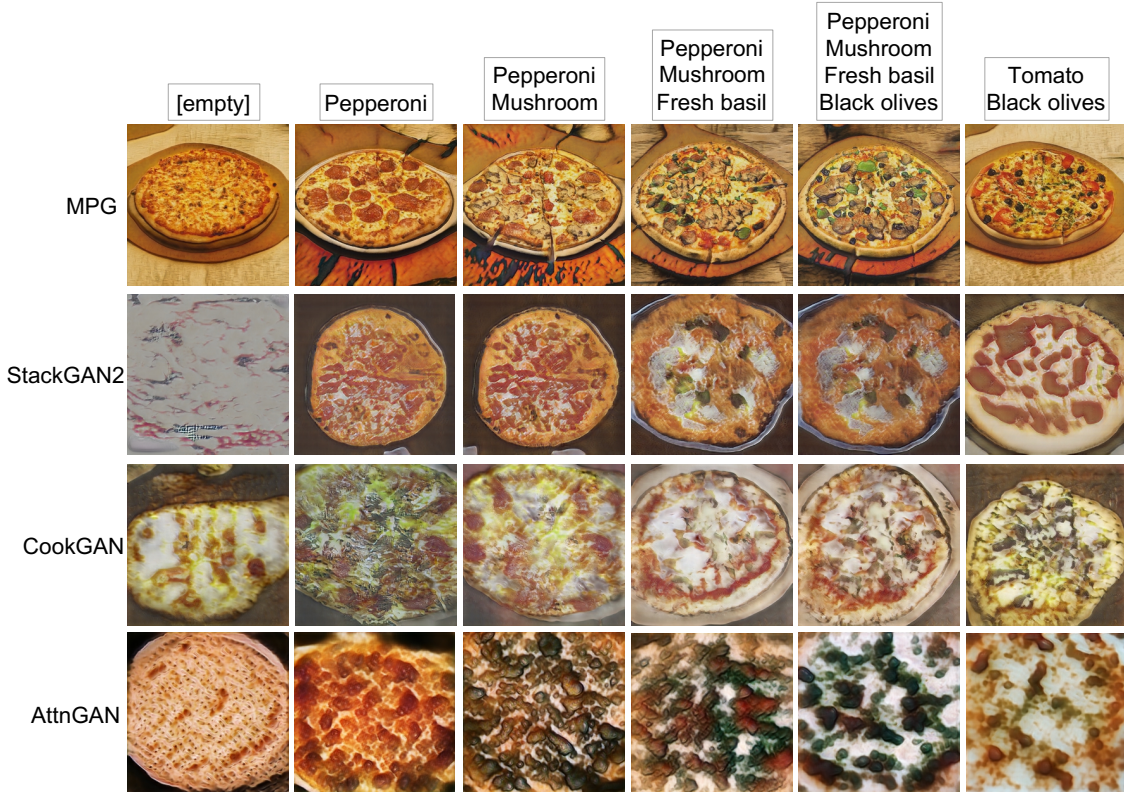


Figure 7. Qualitative comparison between our model *MPG* and baselines

MPG and the baselines, we can see *MPG* has a huge leap forward compared with previous work both in terms of FID and mAP, which means *MPG* not only generates realistic images with diversity but also improves the conditioning on the desired ingredients.

One thing needs to mention is FID has a lower bound which can be estimated from real images, say if we randomly split the real images of **Pizza10** into two image sets (about 5K images each set) and compute the FID between the two sets, we get $FID \approx 8.20$, which means our model still has space to improve. Another thing to note is that mAP is much higher on the generated images from *MPG* even compared with that on real images (0.6804), this sounds unreasonable but we believe since our model is trained with limited data, the images generated is good at capturing the main characteristic of each ingredient and incapable of understanding all possible diversities, while real images could be even harder for the classifier since they contain more variety.

Fig. 7 shows a few samples from our model *MPG* as well as the baselines conditioned on certain ingredient lists. Images generated by *MPG* are more appealing and contain the desired ingredients compared with baselines. Notice how *MPG* can effectively add *Pepperoni*, *Mushroom*, *Fresh basil* and *Black olives* one after another into the gen-

Table 3. Quantitative comparison of performances between *MPG* and its counterparts with missing components

Models	FID↓	mAP↑
<i>MPG</i> -mapping	9.47	0.9799
<i>MPG</i> -SLE	9.29	0.9187
<i>MPG</i> -SLE *	10.03	0.9276
<i>MPG</i> -CR	9.85	0.4712
<i>MPG</i> -uncond	22.26	0.9856
<i>MPG</i>	8.43	0.9816

erated images.

5.2. Ablation Study

To effectively verify the design of *MPG*, we bring out the following experiments. ***MPG*-mapping** removes the mapping network f and directly concatenates scalewise label embedding $\{t_i\}$ with style noise z as the input of the synthesis network. ***MPG*-SLE** removes Scalewise Label Encoder and use the same label embedding for all resolutions. ***MPG*-SLE *** also removes *SLE* and uses the same label embedding for all resolutions, but the label embedding is concatenated with the style noise z before passing through the mapping network, instead of concatenating with w after passing the mapping network. ***MPG*-CR** removes Classification Regularizer. ***MPG*-uncond** removes the unconditional branch in the discriminator.



Figure 8. Images generated from different combinations of ingredient list and style noise. Images in the same row are generated with identical style noise.

Tab. 3 shows the performances of all models, we can observe that mapping network (*MPG-mapping*) and unconditional branch in discriminator (*MPG-uncond*) have impact on FID. Classification Regularizer (*MPG-CR*) mainly affects mAP. And *SLE* influences both FID and mAP.

5.3. Assessment of Generated Images

We provide additional analyses of images created by *MPG*. We first qualitatively study the independence between text embedding and style noise, then we assess the smoothness of the text and the style noise spaces.

Independence. To analyze the independence between text embedding and style noise, we fix the style noise while generating images with different ingredient lists. The result is shown in Fig. 8. Taking the camera position of the images from Noise 1 as the anchor, Noise 2 provides a zoom-in top view, Noise 3 translates the camera position along x-axis, and Noise 4 offers a scaled side view of the pizzas. The likeness of view points in each row and the consistency of ingredients in each column demonstrate the independence between text embedding and style noise.

Smoothness. We verify the smoothness of the learned embedding space and the style noise space by traversing [8]. In Fig. 9, we randomly select two ingredient lists x_1 and x_2 , forward them through *SLE* and obtain the correspond-

ing text embeddings $\{t_i\}_1$ and $\{t_i\}_2$; we then sample two style noise z_1 and z_2 . The traversing is conducted by linear interpolation (e.g. $\{t_i\}_1 \rightarrow \{t_i\}_2$ and $z_1 \rightarrow z_2$).

We can observe the image generated with (*Corn, Pepperoni*) in the top left corner gradually changes to the images containing (*Fresh basil, Black olives*) along the vertical axis, while the view angle and coloring progressively update along the horizontal axis, from z_1 to z_2 . This demonstrates the ability of *MPG* to learn, then recreate independent and smooth major factors of variation in this complex image space.

6. Conclusion

We propose *MPG*, a Multi-ingredient Pizza Generator image synthesis framework, supported by a new **Pizza10** dataset, that can effectively learn to create photo-realistic pizza images from combinations of specified ingredients, as well as manipulate the view point by independently changing the style noise. While extremely effective in visual appearance, the model remains computationally expensive to train and with some loss of detail at fine resolutions, the problems we aim to investigated in future research.

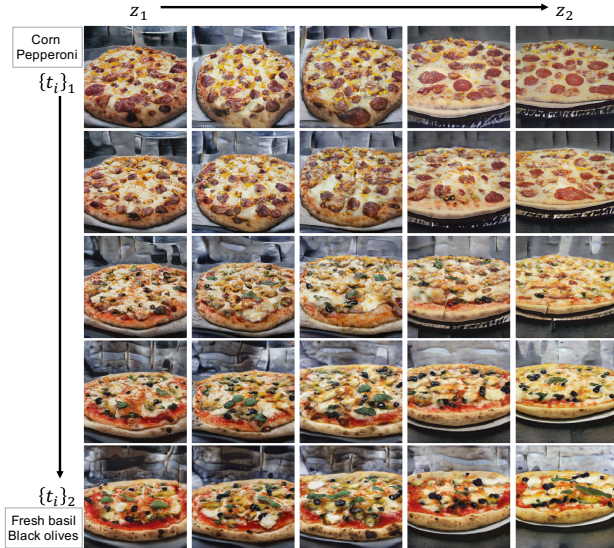


Figure 9. Illustration of traversing through the text embedding space and the style noise space. Images in each row are generated with the same text embedding (interpolated between $\{t_i\}_1$ and $\{t_i\}_2$), while images in each column are synthesized with the same style noise (interpolated between z_1 and z_2).

References

- [1] Martin Arjovsky, Soumith Chintala, and Léon Bottou. Wasserstein gan. *arXiv preprint arXiv:1701.07875*, 2017. 2
- [2] Andrew Brock, Jeff Donahue, and Karen Simonyan. Large scale gan training for high fidelity natural image synthesis. *arXiv preprint arXiv:1809.11096*, 2018. 1, 2
- [3] Yunjey Choi, Minje Choi, Munyoung Kim, Jung-Woo Ha, Sunghun Kim, and Jaegul Choo. Stargan: Unified generative adversarial networks for multi-domain image-to-image translation. In *Proceedings of the IEEE conference on computer vision and pattern recognition*, pages 8789–8797, 2018. 2
- [4] Laurent Dinh, David Krueger, and Yoshua Bengio. Nice: Non-linear independent components estimation. *arXiv preprint arXiv:1410.8516*, 2014. 2
- [5] Laurent Dinh, Jascha Sohl-Dickstein, and Samy Bengio. Density estimation using real nvp. *arXiv preprint arXiv:1605.08803*, 2016. 2
- [6] Harris Drucker and Yann Le Cun. Improving generalization performance using double backpropagation. *IEEE Transactions on Neural Networks*, 3(6):991–997, 1992. 2, 4
- [7] Ori Bar El, Ori Licht, and Netanel Yosephian. Gilt: Generating images from long text. *arXiv preprint arXiv:1901.02404*, 2019. 2
- [8] Ian Goodfellow, Jean Pouget-Abadie, Mehdi Mirza, Bing Xu, David Warde-Farley, Sherjil Ozair, Aaron Courville, and Yoshua Bengio. Generative adversarial nets. In *Advances in neural information processing systems*, pages 2672–2680, 2014. 1, 2, 7
- [9] Ishaan Gulrajani, Faruk Ahmed, Martin Arjovsky, Vincent Dumoulin, and Aaron C Courville. Improved training of wasserstein gans. In *Advances in neural information processing systems*, pages 5767–5777, 2017. 2
- [10] Fangda Han, Ricardo Guerrero, and Vladimir Pavlovic. Cookgan: Meal image synthesis from ingredients. In *The IEEE Winter Conference on Applications of Computer Vision*, pages 1450–1458, 2020. 1, 2, 4, 5, 10, 17
- [11] Kaiming He, Xiangyu Zhang, Shaoqing Ren, and Jian Sun. Deep residual learning for image recognition. In *Proceedings of the IEEE conference on computer vision and pattern recognition*, pages 770–778, 2016. 5
- [12] Zhenliang He, Wangmeng Zuo, Meina Kan, Shiguang Shan, and Xilin Chen. Attgan: Facial attribute editing by only changing what you want. *IEEE Transactions on Image Processing*, 28(11):5464–5478, 2019. 2
- [13] Martin Heusel, Hubert Ramsauer, Thomas Unterthiner, Bernhard Nessler, and Sepp Hochreiter. Gans trained by a two time-scale update rule converge to a local nash equilibrium. In *Advances in neural information processing systems*, pages 6626–6637, 2017. 5
- [14] Phillip Isola, Jun-Yan Zhu, Tinghui Zhou, and Alexei A Efros. Image-to-image translation with conditional adversarial networks. In *Proceedings of the IEEE conference on computer vision and pattern recognition*, pages 1125–1134, 2017. 2
- [15] Yoshifumi Ito, Wataru Shimoda, and Keiji Yanai. Food image generation using a large amount of food images with conditional gan: ramengan and recipegan. In *Proceedings of the Joint Workshop on Multimedia for Cooking and Eating Activities and Multimedia Assisted Dietary Management*, pages 71–74, 2018. 1, 2
- [16] Tero Karras, Timo Aila, Samuli Laine, and Jaakko Lehtinen. Progressive growing of gans for improved quality, stability, and variation. *arXiv preprint arXiv:1710.10196*, 2017. 2
- [17] Tero Karras, Miika Aittala, Janne Hellsten, Samuli Laine, Jaakko Lehtinen, and Timo Aila. Training generative adversarial networks with limited data. *Advances in Neural Information Processing Systems*, 33, 2020. 1, 2
- [18] Tero Karras, Samuli Laine, and Timo Aila. A style-based generator architecture for generative adversarial networks. In *Proceedings of the IEEE conference on computer vision and pattern recognition*, pages 4401–4410, 2019. 1, 2, 5, 12, 13, 14, 15
- [19] Tero Karras, Samuli Laine, Miika Aittala, Janne Hellsten, Jaakko Lehtinen, and Timo Aila. Analyzing and improving the image quality of stylegan. In *Proceedings of the IEEE/CVF Conference on Computer Vision and Pattern Recognition*, pages 8110–8119, 2020. 1, 2, 3
- [20] Durk P Kingma and Prafulla Dhariwal. Glow: Generative flow with invertible 1x1 convolutions. In *Advances in neural information processing systems*, pages 10215–10224, 2018. 2
- [21] Diederik P Kingma and Max Welling. Auto-encoding variational bayes. *arXiv preprint arXiv:1312.6114*, 2013. 2
- [22] Bowen Li, Xiaojuan Qi, Thomas Lukasiewicz, and Philip Torr. Controllable text-to-image generation. In *Advances in*

- Neural Information Processing Systems*, pages 2065–2075, 2019. [2](#)
- [23] Lars Mescheder, Andreas Geiger, and Sebastian Nowozin. Which training methods for gans do actually converge? *arXiv preprint arXiv:1801.04406*, 2018. [2](#)
- [24] Mehdi Mirza and Simon Osindero. Conditional generative adversarial nets. *arXiv preprint arXiv:1411.1784*, 2014. [2](#)
- [25] Takeru Miyato, Toshiki Kataoka, Masanori Koyama, and Yuichi Yoshida. Spectral normalization for generative adversarial networks. *arXiv preprint arXiv:1802.05957*, 2018. [2](#)
- [26] Takeru Miyato and Masanori Koyama. cgans with projection discriminator. *arXiv preprint arXiv:1802.05637*, 2018. [2](#)
- [27] Augustus Odena, Christopher Olah, and Jonathon Shlens. Conditional image synthesis with auxiliary classifier gans. In *International conference on machine learning*, pages 2642–2651, 2017. [4](#)
- [28] Cedric Oeldorf and Gerasimos Spanakis. Loganv2: Conditional style-based logo generation with generative adversarial networks. In *2019 18th IEEE International Conference On Machine Learning And Applications (ICMLA)*, pages 462–468. IEEE, 2019. [2](#)
- [29] Dim P. Papadopoulos, Youssef Tamaazousti, Ferda Ofli, Ingmar Weber, and Antonio Torralba. How to make a pizza: Learning a compositional layer-based gan model. In *The IEEE Conference on Computer Vision and Pattern Recognition (CVPR)*, June 2019. [1](#), [2](#), [4](#)
- [30] Tingting Qiao, Jing Zhang, Duanqing Xu, and Dacheng Tao. Mirrorgan: Learning text-to-image generation by redescription. In *Proceedings of the IEEE Conference on Computer Vision and Pattern Recognition*, pages 1505–1514, 2019. [2](#)
- [31] Andrew Slavin Ross and Finale Doshi-Velez. Improving the adversarial robustness and interpretability of deep neural networks by regularizing their input gradients. *arXiv preprint arXiv:1711.09404*, 2017. [2](#), [3](#), [4](#)
- [32] Mark Sabini, Zahra Abdullah, and Darrith Phan. Gastronomy: Generative cooking with conditional dcgans. [2](#)
- [33] Tim Salimans, Ian Goodfellow, Wojciech Zaremba, Vicki Cheung, Alec Radford, and Xi Chen. Improved techniques for training gans. In *Advances in neural information processing systems*, pages 2234–2242, 2016. [2](#), [3](#), [4](#)
- [34] Amaia Salvador, Nicholas Hynes, Yusuf Aytar, Javier Marin, Ferda Ofli, Ingmar Weber, and Antonio Torralba. Learning cross-modal embeddings for cooking recipes and food images. In *Proceedings of the IEEE conference on computer vision and pattern recognition*, pages 3020–3028, 2017. [4](#), [5](#)
- [35] Ashish Vaswani, Noam Shazeer, Niki Parmar, Jakob Uszkoreit, Llion Jones, Aidan N Gomez, Łukasz Kaiser, and Illia Polosukhin. Attention is all you need. In *Advances in neural information processing systems*, pages 5998–6008, 2017. [4](#)
- [36] Hao Wang, Doyen Sahoo, Chenghao Liu, Ee-peng Lim, and Steven CH Hoi. Learning cross-modal embeddings with adversarial networks for cooking recipes and food images. In *Proceedings of the IEEE Conference on Computer Vision and Pattern Recognition*, pages 11572–11581, 2019. [5](#)
- [37] Su Wang, Honghao Gao, Yonghua Zhu, Weilin Zhang, and Yihai Chen. A food dish image generation framework based on progressive growing gans. In *International Conference on Collaborative Computing: Networking, Applications and Worksharing*, pages 323–333. Springer, 2019. [2](#)
- [38] Thomas Wolf, Lysandre Debut, Victor Sanh, Julien Chaumond, Clement Delangue, Anthony Moi, Pierric Cistac, Tim Rault, Rémi Louf, Morgan Funtowicz, et al. Huggingface’s transformers: State-of-the-art natural language processing. *ArXiv*, pages arXiv–1910, 2019. [4](#)
- [39] Tao Xu, Pengchuan Zhang, Qiuyuan Huang, Han Zhang, Zhe Gan, Xiaolei Huang, and Xiaodong He. Attngan: Fine-grained text to image generation with attentional generative adversarial networks. In *Proceedings of the IEEE conference on computer vision and pattern recognition*, pages 1316–1324, 2018. [2](#), [5](#), [10](#), [18](#)
- [40] Han Zhang, Tao Xu, Hongsheng Li, Shaoting Zhang, Xiaogang Wang, Xiaolei Huang, and Dimitris N Metaxas. Stackgan++: Realistic image synthesis with stacked generative adversarial networks. *IEEE transactions on pattern analysis and machine intelligence*, 41(8):1947–1962, 2018. [2](#), [3](#), [5](#), [10](#), [16](#)
- [41] Jun-Yan Zhu, Taesung Park, Phillip Isola, and Alexei A Efros. Unpaired image-to-image translation using cycle-consistent adversarial networks. In *Proceedings of the IEEE international conference on computer vision*, pages 2223–2232, 2017. [2](#)
- [42] Mu Zhu. Recall, precision and average precision. *Department of Statistics and Actuarial Science, University of Waterloo, Waterloo*, 2:30, 2004. [5](#)

A. Video

In the video¹, we show two examples to demonstrate the main features of our proposed Multi-ingredients Pizza Image Generation (MPG) framework. The first example is an interactive web app we built that shows the images generated from arbitrary selected ingredients and style noise. See Fig. 10 for details about the app layout.

The second example, showcased in Fig. 11, is another interactive web app we designed to explore the smoothness of the learned ingredient representation space. We encourage the reviewers to watch the included video.

B. Additional Visual Comparisons

We provide additional samples from our proposed *MPG* and other state-of-the-art models in Figures 12 through 18. They illustrate:

- Fig. 12 - Fig. 15: Example images generated using our *MPG* under different diversity levels.
- Fig. 16: Example images generated using StackGAN2 [40].
- Fig. 17: Example images generated using CookGAN [10].
- Fig. 18: Example images generated using AttnGAN [39].

¹<https://youtu.be/x3XKXMd1oC8>

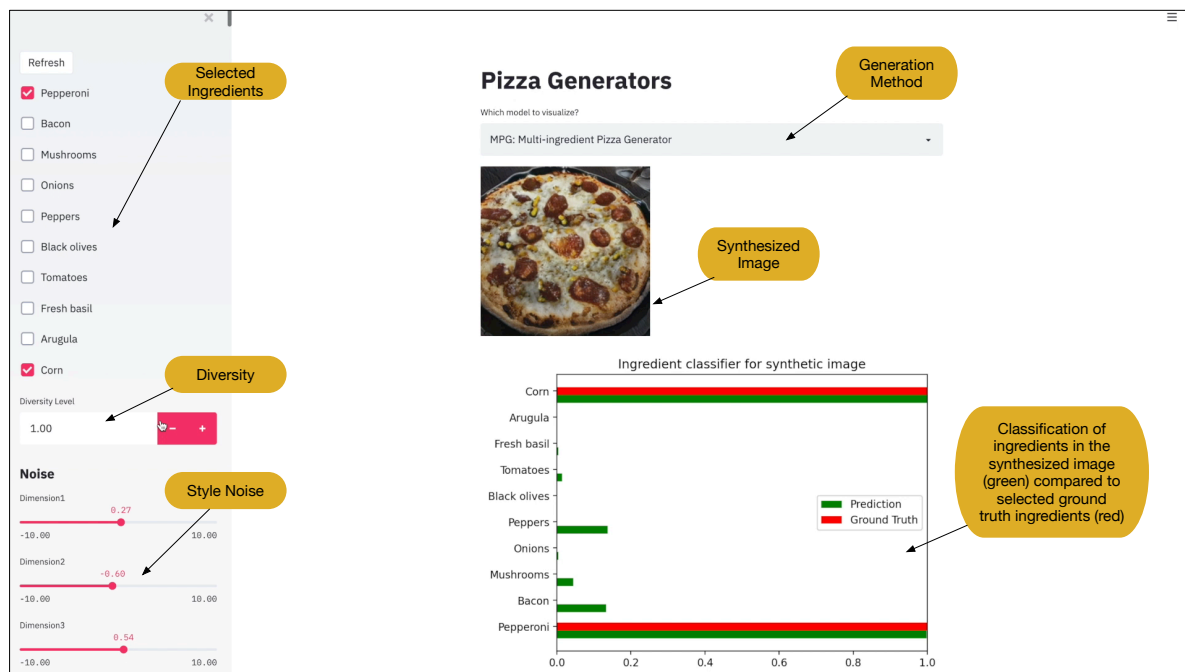


Figure 10. Web app for synthesis of photo-realistic pizza images using the proposed MPG framework. Oval legend blocks explain the main elements used in the demo video.

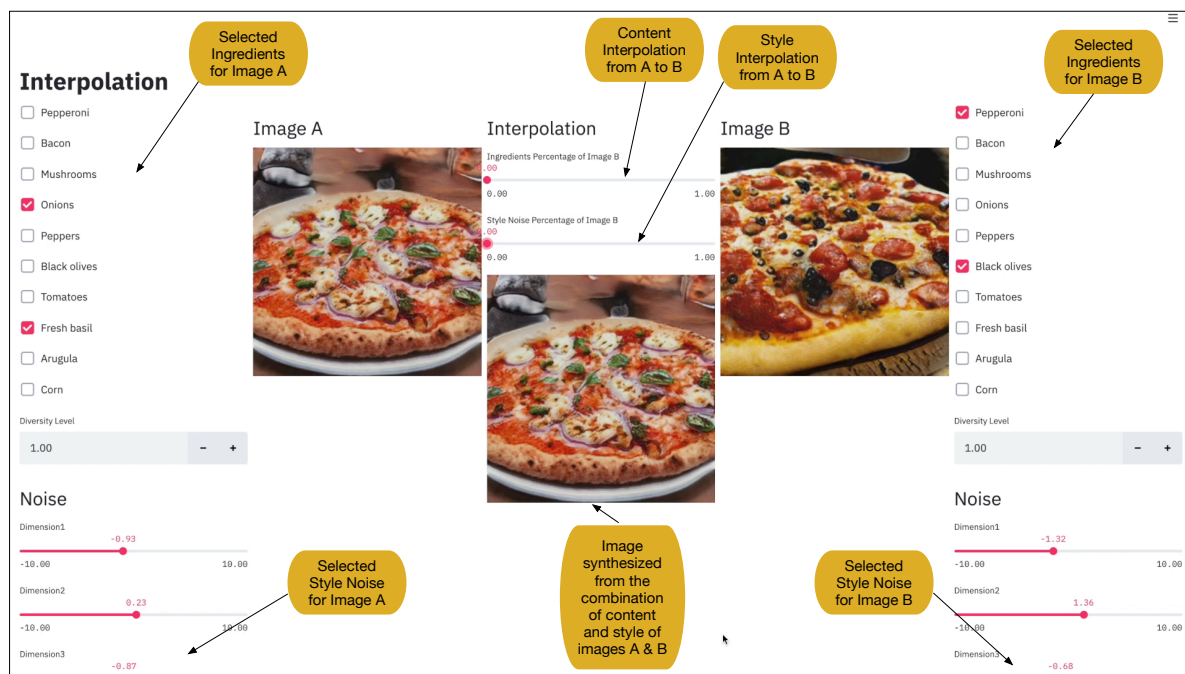


Figure 11. Web app for synthesis of photo-realistic pizza images using the interpolation approach. Image in the middle is created by interpolating the content and the style of used to create the images A and B. Oval legend blocks explain the main elements used in the demo video.



Figure 12. Images generated using our *MPG*, ingredients and style noise are randomly sampled. The ingredients are shown on top left corner in each image. The diversity level (e.g. truncation) is set to be 1.00. Please check [18] for how to accomplish this using the truncation trick.



Figure 13. Images generated using our *MPG*, ingredients and style noise are randomly sampled. The ingredients are shown on top left corner in each image. The diversity level (e.g. truncation) is set to be 0.75. Please check [18] for how to accomplish this using the truncation trick.



Figure 14. Images generated using our *MPG*, ingredients and style noise are randomly sampled. The ingredients are shown on top left corner in each image. The diversity level (e.g. truncation) is set to be 0.50. Please check [18] for how to accomplish this using the truncation trick.



Figure 15. Images generated using our *MPG*, ingredients and style noise are randomly sampled. The ingredients are shown on top left corner in each image. The diversity level (e.g. truncation) is set to be 0.25. Please check [18] for how to accomplish this using the truncation trick.



Figure 16. Images generated using StackGAN2 [40], ingredients and style noise are randomly sampled. The ingredients are shown on top left corner in each image.



Figure 17. Images generated using CookGAN [10], ingredients and style noise are randomly sampled. The ingredients are shown on top left corner in each image.



Figure 18. Images generated using AttnGAN [39], ingredients and style noise are randomly sampled. The ingredients are shown on top left corner in each image.